



## Contrasting lithium and magnesium isotope fractionation during continental weathering

Fang-Zhen Teng<sup>a,\*</sup>, Wang-Ye Li<sup>a,b</sup>, Roberta L. Rudnick<sup>c</sup>, L. Robert Gardner<sup>d</sup>

<sup>a</sup> Isotope Laboratory, Department of Geosciences & Arkansas Center for Space and Planetary Sciences, University of Arkansas, Fayetteville, AR 72701, USA

<sup>b</sup> CAS Key Laboratory of Crust–Mantle Materials and Environments, School of Earth and Space Sciences, University of Science and Technology of China, Hefei, Anhui 230026, China

<sup>c</sup> Geochemistry Laboratory, Department of Geology, University of Maryland, College Park, MD 20742, USA

<sup>d</sup> Department of Geology, University of South Carolina, Columbia, SC 29208, USA

### ARTICLE INFO

#### Article history:

Received 23 April 2010

Received in revised form 20 September 2010

Accepted 22 September 2010

Available online 20 October 2010

Editor: R.W. Carlson

#### Keywords:

lithium  
magnesium  
isotope fractionation  
continental weathering

### ABSTRACT

Magnesium isotopic compositions of a profile through saprolites developed on a diabase dike from South Carolina have been measured in order to study the behavior of Mg isotopes during continental weathering. As weathering progresses, Mg isotopes are greatly fractionated and are correlated with Mg concentration, clay mineral proportions and density of the saprolites.  $\delta^{26}\text{Mg}$  values increase from  $-0.22$  in the unweathered diabase to  $+0.65$  in the most weathered saprolite. These observations are consistent with the release of light Mg to the hydrosphere and formation of isotopically heavy Mg in the weathered products. The loss of Mg during weathering can be modeled by Rayleigh distillation with an apparent fractionation factor between the saprolite and fluid ( $\alpha$ ) of 1.00005 to 1.0004, i.e., up to 0.4‰ fractionation in the  $^{26}\text{Mg}/^{24}\text{Mg}$  ratio between the saprolite and fluid. The large variation in  $\alpha$  value reflects a mineralogical control on Mg isotope fractionation during primary dissolution of Mg-rich minerals and formation of secondary minerals during continental weathering. Like Mg isotopes, Li isotopes in the saprolite profile are also greatly fractionated, with  $\delta^7\text{Li}$  values ranging from  $-6.7$  down to  $-20$ . The large Li isotope fractionation and variation in Li concentration, as well as irregularities in the  $\delta^7\text{Li}$  profile with depth, however, cannot be explained by Li loss during weathering alone. Instead, Li can be modeled by a two-step process: (1) equilibrium isotope fractionation during continental weathering, which lowered  $\delta^7\text{Li}$  and Li concentrations and produced a Li concentration gradient in the saprolites like that seen in Mg, and (2) subsequent kinetic isotope fractionation produced by diffusion of Li in the saprolites, possibly across a paleo-water table. The results presented here suggest that continental weathering will shift the Mg isotopic composition of the continental crust to values higher than the mantle value, whereas crustal recycling over the history of the Earth will have no discernible effect on the Mg isotopic composition of the mantle.

© 2010 Elsevier B.V. All rights reserved.

### 1. Introduction

Continental weathering is a geochemical link between the outer parts of the Earth i.e., atmosphere, hydrosphere and continents. For example, chemical weathering on the continents and deposition of limestones sequester  $\text{CO}_2$  and regulate the  $\text{CO}_2$  content of the atmosphere (Urey, 1952). Furthermore, chemical weathering leads to the decomposition of rocks and the release of elements from continents into solution. It may be one of the processes that shifts the composition of the continental crust from basaltic to andesitic (Albarede, 1998; Anderson, 1982; Lee et al., 2008). It also controls the chemical composition of river waters, which further influences the composition of seawater (Edmond et al., 1979).

Two types of natural samples have generally been used to study continental weathering (Kump et al., 2000, and references therein): chemical weathering profiles and river waters. Studies of chemical weathering profiles developed on different types of rocks in different climates demonstrate how chemical weathering affects mineral dissolution, secondary phase crystallization, elemental transport and isotope fractionation as a function of mineralogy of the protolith, the supply of water, temperature, humidity and other chemical and physical conditions. Such studies date back to 1938 when Goldich (1938) systematically investigated the relative susceptibility of common rock-forming minerals to weathering and the behavior of elements in a weathering profile developed on an Archean granite gneiss. On the other hand, studies of rivers can yield the rates of chemical erosion and indirectly reflect the mineral compositions of rocks that are the source of the river loads, as well as climate, topography and other chemical and physical conditions (Berner and Berner, 1987; Drever, 1997).

\* Corresponding author. Department of Geosciences, University of Arkansas, Fayetteville, AR 72701, USA. Tel.: +1 479 575 4524; fax: +1 479 575 3469.

E-mail address: [fteng@uark.edu](mailto:fteng@uark.edu) (F.-Z. Teng).

Magnesium is a water-soluble major element that occurs in the hydrosphere, continental crust and the mantle. Magnesium has three stable isotopes ( $^{24}\text{Mg}$ ,  $^{25}\text{Mg}$  and  $^{26}\text{Mg}$ ), the study of which, during continental weathering, may help to document the interactions between hydrosphere, crust and mantle. Whereas the mantle has  $\delta^{26}\text{Mg} = -0.25 \pm 0.1$  (Dauphas et al., 2010; Handler et al., 2009; Teng et al., 2007, 2010; Yang et al., 2009), the upper continental crust, as sampled by shales, loess and granites, is quite heavy, with  $\delta^{26}\text{Mg}$  up to  $+0.92$  (Li et al., 2010; S.-A. Liu et al., 2010; Shen et al., 2009). This isotopically heavy composition has been attributed to continental weathering, with light Mg partitioned into water, leaving heavy Mg behind in the residue. The Mg isotopic composition of seawater is light and homogenous with  $\delta^{26}\text{Mg} = -0.8 \pm 0.1$  (Chang et al., 2003; de Villiers et al., 2005; Teng et al., 2010; Young and Galy, 2004), consistent with the relatively long residence time for Mg in the oceans (Li, 1982).  $\delta^{26}\text{Mg}$  of river waters is more variable, and, on average, lighter than that of the seawater and mantle, reflecting heterogeneous source rocks and Mg isotope fractionation during continental weathering (Brenot et al., 2008; de Villiers et al., 2005; Pogge Von Strandmann et al., 2008a,b; Tipper et al., 2006a,b; 2008). When compared to Mg, the isotope geochemistry of Li is better understood. The mantle has  $\delta^7\text{Li} = +4$  (Jeffcoate et al., 2007; Magna et al., 2006; Seitz et al., 2004) whereas the seawater is heavy with  $\delta^7\text{Li} = +32$  (Chan and Edmond, 1988). By contrast, both the upper and deep continental crusts are highly heterogeneous and isotopically light (Teng et al., 2004, 2008, 2009). The isotopically light composition of the continental crust is inferred to result from weathering, with heavy Li isotopes lost into the hydrosphere, leaving lighter Li behind in the weathered residue (Teng et al., 2004, 2008, 2009). This interpretation is supported by studies of weathering profiles and river waters (Huh et al., 2004; Kisakurek et al., 2004, 2005; Pistiner and Henderson, 2003; Pogge Von Strandmann et al., 2008b; Rudnick et al., 2004).

While several studies have been performed on the Mg isotopic compositions of river waters, to our knowledge, no systematic study has yet been made on weathering profiles. Here we report Mg isotopic data for a profile through well-characterized saprolites developed on a subvertical Mesozoic diabase dike, South Carolina (Gardner et al., 1981). The bulk composition, mineralogy and bulk density of this saprolite profile were previously determined by Gardner and colleagues (Gardner and Kheoruenromne, 1980; Gardner et al., 1981), allowing one to evaluate the effects of chemical weathering directly. In addition, previous studies of Li isotopes in this saprolite revealed significant isotope fractionation (Rudnick et al., 2004), which we re-evaluate here.

Our results show that the degree of Mg isotope fractionation increases directly with the intensity of chemical weathering, with the preferential loss of light Mg into the hydrosphere, resulting in extremely high  $\delta^{26}\text{Mg}$  values (up to  $+0.65$ ) in the residue. By contrast, Li isotopes show an irregular change with weathering intensity, which likely reflects the influence of kinetic isotope fractionation superimposed upon Rayleigh distillation. These findings demonstrate that diffusion-driven fractionation of Li isotopes can occur during low-temperature water–rock interactions and that, over time, continental weathering shifts the stable isotopic compositions of the continental crust away from the mantle values.

## 2. Samples

The saprolites in this study formed during the Tertiary in a humid, subtropical climate and are developed on a Mesozoic greenschist facies diabase dike that cuts granite in Cayce, South Carolina (N33° 58.09', and W81° 03.07') (Gardner et al., 1981). The diabase dike is exposed in the walls of a quarry, overlain by a thin (~2 m) layer of coastal plain sediment, and is approximately 7 m wide, with saprolites developed within the top 11 m (Fig. 1) (Gardner et al., 1981). Unweathered diabase crops out below 11 m and contains significant amounts of talc

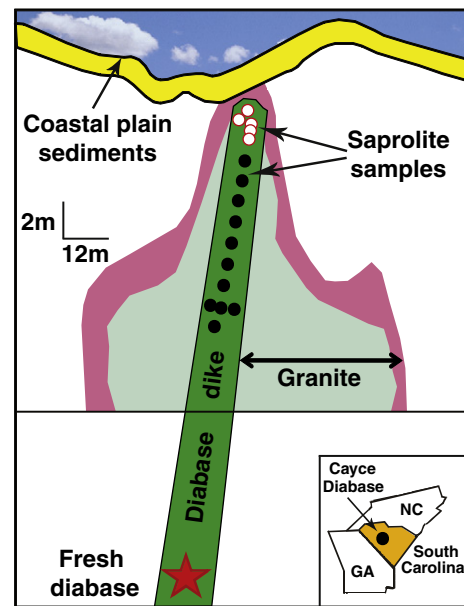


**Fig. 1.** Sketch of cross-section through granite quarry wall near Cayce, South Carolina, showing diabase dike mantled by alteration halo surrounding granite saprolite. Light green depicts region of green-stained granite whereas light red represents region of red-stained granite. Horizontal line marks a change in vertical scale. Star represents unweathered diabase; and open circles represent samples at or above 2 m depth and closed circles are samples below 2 m. Inset shows sample locality for diabase outcrop. From Rudnick et al. (2004), after Gardner et al. (1981).

(20%) and chlorite (8%), in addition to plagioclase (40%), clinopyroxene (29%) and opaque minerals (3%) (Gardner et al., 1981). Green- and red-stained alteration haloes occur sequentially within the granite surrounding the dike. These form a rather narrow (3–6 m thick) aureole in the upper 6 m of the profile, but increase in thickness up to ~30 m below 6 m depth (Fig. 1).

Fresh saprolite samples were collected along a vertical profile through the center of the dike (Fig. 1), pulverized and analyzed for density, clay mineral proportions and bulk composition (Gardner et al., 1981). The weathering intensity is greatest at the shallowest level, where the greatest amount of leaching occurred due to rainwater infiltration, and falls off with depth (Fig. 2). Talc and chlorite were weathered first, followed by clinopyroxene and plagioclase. Kaolinite, smectite and Fe-oxides are the main secondary minerals that formed in the saprolites during the weathering (Fig. 2).

A discontinuity in clay mineralogy and bulk chemistry exists at a depth of ~2 m of the weathering profile (Gardner and Kheoruenromne, 1980; Gardner et al., 1981). Below the discontinuity, siderite veins have developed by weathering of original chlorite veins in the diabase and the kaolinite to smectite ratio increases as the weathering intensity increases and bulk density decreases towards the discontinuity (Fig. 2). These mineralogical changes reflect dissolution of chlorite, talc, clinopyroxene and plagioclase and formation of kaolinite and smectite, as well as transformation of smectite to kaolinite during progressing weathering. Above the discontinuity, no siderite veins formed, the kaolinite/smectite ratio and bulk density are roughly constant (Fig. 2), and kaolinite and smectite contents decrease with the decreasing density towards the surface (Gardner et al., 1981). Gardner et al. (1981) interpreted the discontinuity as a result of a change in redox: the upper profile was more oxidized, as reflected in the lack of siderite and by greater amounts of Fe-rich smectite compared to kaolinite, while the lower portion of the profile was more reduced, as reflected in the formation of siderite and formation of kaolinite over Al-rich smectite. Chemical compositions of saprolites also reflect these mineralogical changes at the 2 m discontinuity (Fig. 2). Furthermore, below the 2 m depth, chemical and Li isotopic compositions show a

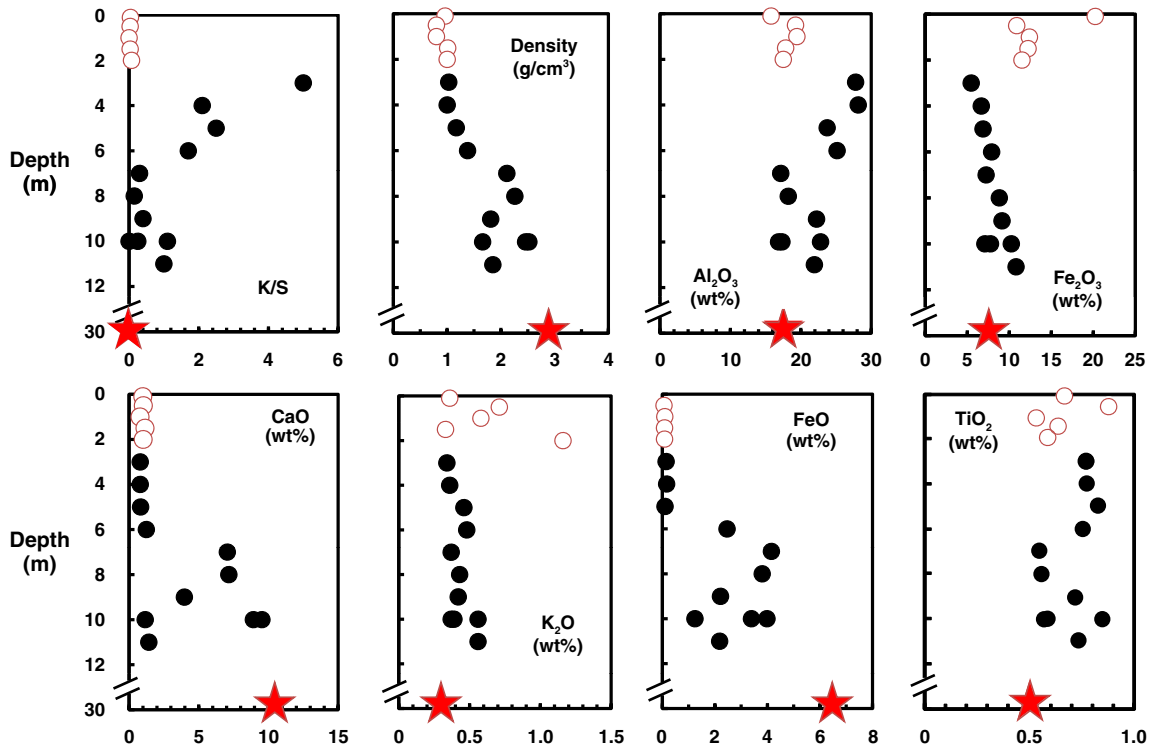


**Fig. 2.** K/S (kaolinite/smectite) ratio, bulk density and selected element concentrations of saprolites as a function of depth. Star represents unweathered diabase; and open circles represent samples at or above 2 m depth and closed circles are samples below 2 m. Data are reported in Table 2.

discontinuity at 6 m depth, which was interpreted to reflect the former presence of a water table at this depth (Gardner et al., 1981; Rudnick et al. 2004).

Sixteen saprolite samples from the 11 m weathering profile and one fresh diabase from 30 m below were analyzed for Mg isotopic compositions. The mineralogy, major and trace element geochemistry and Li isotope geochemistry of these samples were previously reported (Gardner et al., 1981; Rudnick et al., 2004).

### 3. Analytical methods

Magnesium isotopic analyses were performed at the Isotope Laboratory of the University of Arkansas, Fayetteville. Procedures for sample dissolution, column chemistry and instrumental analysis are similar to those reported in previous studies (Li et al., 2010; S.-A. Liu et al., 2010; Teng et al., 2010; Yang et al., 2009). Only a brief description is given below.

Samples were dissolved in Savillex screw-top beakers in a mixture of concentrated HF–HNO<sub>3</sub>–HCl. Separation of Mg was achieved by cation exchange chromatography with Bio-Rad 200–400 mesh AG50W-X8 resin in 1 N HNO<sub>3</sub> media. Samples containing ~50 μg of Mg were loaded on the resin and eluted by 1 N HNO<sub>3</sub> with Mg yield close to 100%. This procedure was repeated in order to obtain a pure Mg solution for mass spectrometry. At least two standards were processed with unknown samples for each batch of column chemistry.

Magnesium isotopic compositions were analyzed by the standard bracketing method using a Nu Plasma MC-ICP-MS at the University of Arkansas. Magnesium isotope data are reported in standard  $\delta$ -notation in per mil relative to DSM3 (Galy et al., 2003):

$$\delta^X \text{Mg} = 10^3 \times \left\{ \frac{(^X \text{Mg}/^{24} \text{Mg})_{\text{sample}}}{(^X \text{Mg}/^{24} \text{Mg})_{\text{DSM3}}} - 1 \right\}$$

where X refers to 25 or 26.

At least one standard was routinely analyzed during the course of an analytical session. The precision on the measured <sup>26</sup>Mg/<sup>24</sup>Mg ratio, based on  $\geq 4$  repeat runs of the same sample solution during a single analytical session, is  $< \pm 0.1\%$  (2SD) (Teng et al. 2010). Multiple analyses of IL-Mg-1, a synthetic solution with concentration ratios of Mg:Fe:Al:Ca:Na:K:Ti = 1:1:1:1:1:1:0.1, yield  $\delta^{26}\text{Mg}$  of +0.04, 0 and –0.02 (Table 1), within uncertainties of the expected value of  $0 \pm 0.1$  (2SD). Results for solution, rock and mineral standards analyzed during the course of this study (Table 1) also agree with previously published data (Chang et al., 2003; Galy et al., 2003; Teng et al., 2010; Young and Galy, 2004).

### 4. Results

Magnesium isotopic compositions are reported in Table 1 for solution, mineral and rock reference materials and Table 2 for the

**Table 1**  
Magnesium isotopic compositions of reference materials.

Standard	Type	$\delta^{26}\text{Mg}$	2SD	$\delta^{25}\text{Mg}$	2SD
Cambridge 1		–2.61	0.08	–1.35	0.06
Replicate		–2.62	0.07	–1.35	0.06
IL-Mg-1	Synthetic	+0.04	0.06	+0.05	0.06
Replicate		0	0.05	–0.01	0.06
Replicate		–0.02	0.09	–0.01	0.06
Hawaii seawater		–0.81	0.07	–0.42	0.05
Replicate		–0.86	0.05	–0.45	0.02
KH	Olivine	–0.26	0.10	–0.14	0.05
Replicate		–0.29	0.04	–0.17	0.03
Allende	Chondrite	–0.28	0.10	–0.17	0.07
Replicate		–0.32	0.08	–0.15	0.04
DTS-1	Dunite	–0.30	0.09	–0.13	0.05
DTS-2	Dunite	–0.33	0.05	–0.16	0.06

2SD = 2 times the standard deviation of the population of n repeat measurements of a sample solution. IL-Mg-1 is a synthetic solution with concentration ratios of Mg:Fe:Al:Ca:Na:K:Ti = 1:1:1:1:1:1:0.1. Replicate refers to repeat column chemistry and measurement of different aliquots of a stock solution.

**Table 2**  
Major element composition, bulk density and Mg isotopic composition of saprolites and fresh Cayce diabase from South Carolina.

Sample	Depth (m)	Density (g/cm <sup>3</sup> )	K/S	Al <sub>2</sub> O <sub>3</sub> (wt.%)	Fe <sub>2</sub> O <sub>3</sub> (wt.%)	FeO (wt.%)	MgO (wt.%)	CaO (wt.%)	K <sub>2</sub> O (wt.%)	TiO <sub>2</sub> (wt.%)	Li (ppm)	δ <sup>7</sup> Li	MgO (norm)	δ <sup>26</sup> Mg	2SD	δ <sup>25</sup> Mg	2SD
M1	0.1	1.0	0.04	15.8	20.2		1.8	1.0	0.36	0.66	5.1	-11.6	0.11	+0.53	0.11	+0.28	0.08
M3	0.5	0.8	0.03	19.3	10.9	0.1	2.2	1.0	0.71	0.88	7.1	-10.1	0.10	+0.62	0.11	+0.32	0.08
M4	1.0	0.8	0.00	19.5	12.4	0.1	1.6	0.8	0.58	0.52	8.2	-13.3	0.13	+0.65	0.11	+0.35	0.08
M5	1.5	1.0	0.03	17.9	12.2	0.1	2.0	1.1	0.33	0.64	5.6	-14.4	0.13	+0.59	0.11	+0.31	0.08
M6	2.0	1.0	0.07	17.5	11.5	0.1	2.0	1.0	1.16	0.58	9.6	-12.1	0.14	+0.61	0.09	+0.31	0.04
M7	3.0	1.0	5.00	27.8	5.5	0.1	0.6	0.8	0.34	0.77	20.0	-13.8	0.03	+0.30	0.09	+0.15	0.04
Replicate														+0.22	0.07	+0.12	0.04
M8	4.0	1.0	2.10	28.2	6.7	0.2	0.9	0.8	0.36	0.78	18.0	-17.1	0.05	+0.42	0.09	+0.23	0.04
M9	5.0	1.2	2.50	23.8	6.9	0.1	1.0	0.8	0.46	0.81	14.0	-17.3	0.05	+0.40	0.09	+0.22	0.04
M10	6.0	1.4	1.70	25.2	7.9	2.5	1.0	1.2	0.48	0.76	24.0	-20.2	0.05	+0.07	0.07	+0.02	0.04
Replicate														+0.11	0.10	+0.03	0.04
M11	7.0	2.1	0.30	17.2	7.2	4.2	11.9	7.1	0.37	0.55	47.0	-6.7	0.88	-0.17	0.07	-0.10	0.04
M12	8.0	2.3	0.15	18.2	8.8	3.8	8.6	7.2	0.43	0.56	23.0	-10.4	0.62	-0.11	0.07	-0.04	0.04
M13	9.0	1.8	0.40	22.2	9.1	2.2	5.5	4.0	0.42	0.72	42.0	-11.8	0.31	+0.02	0.07	+0.02	0.04
M14	10.0	1.7	1.10	22.8	10.2	1.2	2.7	1.2	0.56	0.85	42.0	-9.7	0.13	-0.12	0.07	-0.05	0.04
L14-8	10.0	2.5	0.25	17.3	7.8	3.4	11.0	8.9	0.37	0.57	56.0	-9.1	0.78	-0.13	0.07	-0.08	0.04
L14-9	10.0	2.5	0.00	16.9	7.1	4.0	10.5	9.5	0.39	0.58	32.0	-8.1	0.73	-0.31	0.08	-0.17	0.05
M15	11.0	1.9	1.00	21.9	10.8	2.2	5.8	1.4	0.56	0.73	24.0	-13.7	0.32	-0.19	0.07	-0.08	0.04
M20	30.0	3.0	0.00	17.1	7.1	6.3	11.8	10.4	0.32	0.48	23.0	-4.4	1.00	-0.22	0.07	-0.12	0.04

Sample M20 is the unweathered diabase protolith while all other samples are saprolites. Depth, bulk densities, K/S and major element data are from Gardner et al. (1981), where K/S=kaolinite/smectite intensity ratio analyzed from XRD and FeO concentration was determined by titration. Li and δ<sup>7</sup>Li data are from Rudnick et al. (2004). δ<sup>7</sup>Li = [(<sup>7</sup>Li/<sup>6</sup>Li)<sub>sample</sub> / (<sup>7</sup>Li/<sup>6</sup>Li)<sub>L-SVEC</sub> - 1] × 1000, where L-SVEC is Li standard that is made from Li<sub>2</sub>CO<sub>3</sub> (Flesch et al., 1973). Normalized MgO concentration, which is [MgO/TiO<sub>2</sub>]<sub>saprolite</sub> / [MgO/TiO<sub>2</sub>]<sub>protolith</sub>, is used here to evaluate the mobility of Mg relative to Ti. Replicate refers to repeat column chemistry and measurement of different aliquots of a stock solution.

saprolites and unweathered diabase. For reference, major element, Li concentration and isotopic data, bulk density and the kaolinite/smectite (K/S) ratio analyzed by Gardner et al. (1981) and Rudnick et al. (2004) are also included in Table 2.

Magnesium, like most other elements, shows a concentration discontinuity at 2 m, and at 6 m depth (Fig. 3) in the weathering profile. Above the 2 m discontinuity, Mg concentrations are more or less constant at ~0.12 (normalized to Ti, Fig. 3). Below this, Mg concentrations are uniformly low, but they increase dramatically and non-uniformly below 6 m. The unweathered diabase, at 30 m depth, has the highest Mg concentration.

Magnesium isotopic compositions decrease systematically with depth and bulk density over the whole weathering profile (Fig. 3). The shallowest saprolites have the lowest bulk density and the heaviest

isotopic composition (δ<sup>26</sup>Mg = +0.65) while saprolites at the bottom have the highest bulk density and the lightest isotopic composition (δ<sup>26</sup>Mg = -0.31). The unweathered diabase has Mg isotopic composition similar to the least weathered overlying saprolite, as well as those of unweathered oceanic basalts (Teng et al., 2007, 2010; Wiechert and Halliday, 2007) (Fig. 4).

Lithium concentrations increase with depth, with very low Li concentrations (5 ppm) near the surface increasing to variable but high concentrations (up to 56 ppm) deep within the profile (Rudnick et al., 2004). The unweathered diabase has a Li concentration (23 ppm) falling between the two extremes (Table 2, Fig. 5). Lithium isotopic composition is also highly variable, with δ<sup>7</sup>Li ranging from -6.7 to -20 in the saprolites (Rudnick et al., 2004). Unlike the Li concentration, δ<sup>7</sup>Li, however, does not vary systematically with depth

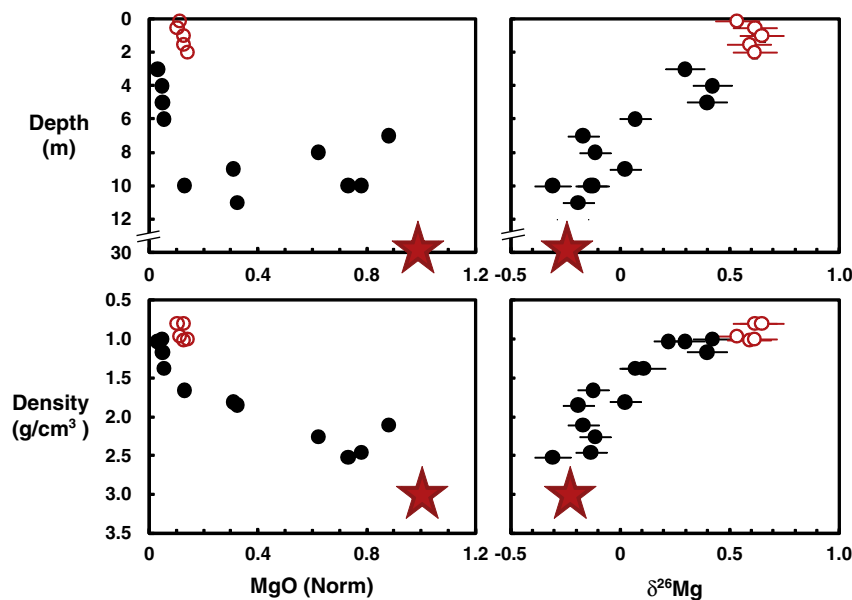


**Fig. 3.** Magnesium concentration normalized to titanium (see Table 2 for normalization procedure) and δ<sup>26</sup>Mg as a function of depth and bulk density for the diabase weathering profile. Error bars represent 2SD uncertainties. Star represents unweathered diabase; and open circles represent samples at or above 2 m depth and closed circles are samples below 2 m. Data are reported in Table 2.

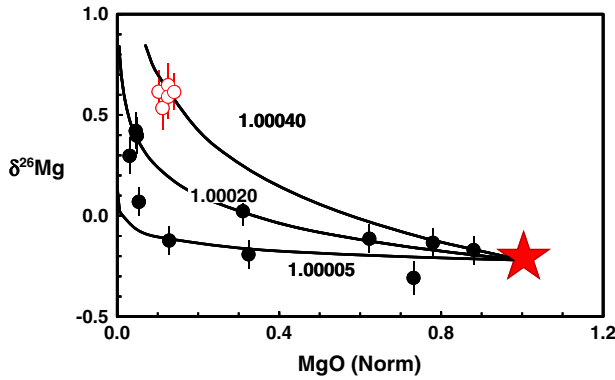


**Fig. 4.** Magnesium concentration normalized to titanium vs.  $\delta^{26}\text{Mg}$  for saprolite profile. Curved lines depict Mg removal via Rayleigh distillation for different values of the fractionation factor  $\alpha$  [ $\alpha = (^{26}\text{Mg}/^{24}\text{Mg})_{\text{saprolite}} / (^{26}\text{Mg}/^{24}\text{Mg})_{\text{fluid}}$ ]. Rayleigh distillation equation:  $\delta^{26}\text{Mg}_{\text{saprolite}} = (\delta^{26}\text{Mg}_{\text{diabase}} + 1000)f^{\alpha-1} - 1000$ ;  $f$ : the fraction of Mg remaining in the rock, calculated from  $\text{Mg}_{\text{saprolite}}/\text{Mg}_{\text{diabase}}$ . Star represents unweathered diabase; and open circles represent samples at or above 2 m depth and closed circles are samples below 2 m. Error bars represent 2SD uncertainties. Data are reported in Table 2.

but rather shows a step function, with a discontinuity at 6 m depth (Fig. 5). The unweathered diabase has the highest  $\delta^7\text{Li}$  (−4.3).

## 5. Discussion

In this section, we first discuss the behavior of Mg isotopes during continental weathering, reinterpret the Li isotopic profile in this suite of saprolites, and finally calculate the influence of weathering on the Mg isotopic composition of the continental crust and the mantle.

### 5.1. Magnesium isotope fractionation during weathering

Magnesium is fluid-mobile and is released into the water during continental weathering when Mg-rich minerals break down and

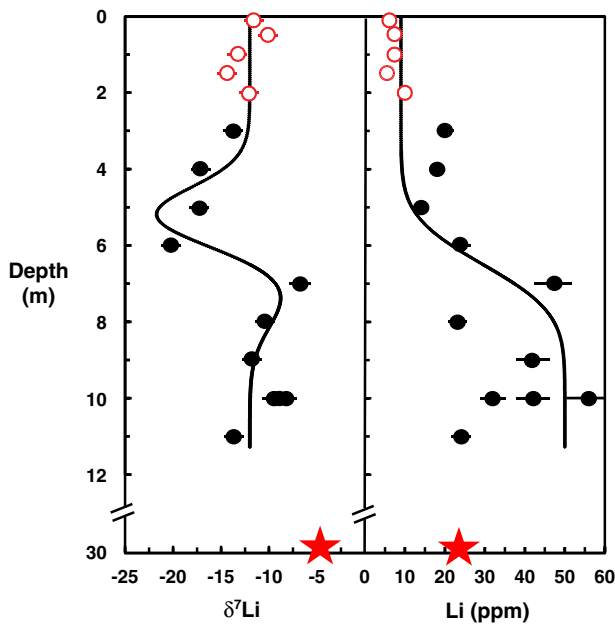


**Fig. 5.** Diffusion models (solid lines) showing the effects of Li diffusion from a Li-rich layer below 6 m depth upwards into the Li-poor saprolite above. This depth may mark the position of a paleo-water table (Rudnick et al., 2004). Star represents unweathered diabase; and open circles represent samples at or above 2 m depth and closed circles are samples below 2 m. Error bars represent 2SD uncertainties. Lithium data are from Rudnick et al. (2004). See text for details.

secondary minerals form. During this process, Mg is redistributed between crust and hydrosphere, potentially coupled with large isotope fractionation. The correlation between Mg concentrations and isotopic compositions in the saprolite profile (Fig. 4) indicates significant Mg isotope fractionation and Mg loss during chemical weathering.

Inter-mineral Mg isotope fractionation in igneous rocks is generally limited (e.g.,  $\Delta^{26}\text{Mg}_{\text{Hbl}-\text{Bt}} = -0.06 \pm 0.08$ , 2SD, S.-A. Liu et al., 2010). Minerals in the diabase are, thus, expected to have similar Mg isotopic compositions, therefore differential weathering of Mg-host minerals in the diabase can be ruled out as a cause of the variations in  $\delta^{26}\text{Mg}$ . The isotope fractionation in the saprolite, thus, must be associated with primary dissolution of diabase and formation of secondary minerals during weathering. It is difficult to evaluate the exact role of these two processes in controlling Mg isotopic compositions of the saprolites since little is known about the behavior of Mg isotopes during primary dissolution of pyroxene, talc and chlorite and formation of clay minerals like smectite and kaolinite during continental weathering. The correlated MgO and  $\delta^{26}\text{Mg}$  in the saprolite, however suggest isotope fractionation accompanied Mg loss during weathering. The Mg loss indicates that the amount of Mg released into fluids during primary dissolution of Mg-rich minerals in the diabase exceeded the amount of Mg uptake into the secondary minerals.

The Mg loss can be modeled by Rayleigh distillation, with light Mg isotopes preferring fluids to saprolites and with various apparent fractionation factors between saprolite and fluid [ $\alpha = (^{26}\text{Mg}/^{24}\text{Mg})_{\text{saprolite}} / (^{26}\text{Mg}/^{24}\text{Mg})_{\text{fluid}}$ ] (Fig. 4). The apparent  $\alpha$  values vary from 1.00005 to 1.0004 (Fig. 4), which corresponds to a change of Mg isotope fractionation between saprolite and fluid from 0.05‰ up to 0.4‰. The large range in  $\alpha$  values reflects the complex effects of both dissolution of Mg-rich minerals and formation of secondary minerals on Mg isotopic compositions of the saprolite. Although it is difficult to evaluate the effect of dissolution of primary minerals on controlling Mg isotopic compositions of the saprolites since most of these primary minerals reacted out, our data clearly indicate that formation of secondary minerals plays a significant role. For example, saprolites above the 2 m discontinuity fall near the Rayleigh distillation curves with higher apparent  $\alpha$  value, whereas those below the 2 m discontinuity fall near the Rayleigh distillation curves with lower apparent  $\alpha$  values. This discontinuity is interpreted as a change in redox (Gardner et al., 1981). The upper 2 m of the profile has greater amounts of Fe (Mg)-rich smectite compared to kaolinite, i.e., a lower kaolinite/smectite ratio, while the lower portion of the profile has more kaolinite over Al-rich smectite. Since smectite is the main Mg-host mineral in the saprolites of the upper profile, the larger  $\alpha$  values may therefore reflect larger fractionation factors between smectite and fluid than those between kaolinite/other minerals and fluids.

Nonetheless, in order to fully understand how Mg isotopes behave during weathering in different climates and for different types of rocks, more studies on the direction, magnitude and mechanism of Mg isotope fractionation between minerals and fluids during primary dissolution of different types of rocks and formation of various secondary minerals are needed.

### 5.2. Diffusion-driven Li isotope fractionation during weathering

Rudnick et al. (2004) measured Li concentrations and isotopic compositions of the saprolites and show that Li isotopic compositions of the saprolites are always lighter than that of the unweathered diabase (Fig. 5), suggesting a preference of light Mg in the residue. Unlike the Mg isotopes,  $\delta^7\text{Li}$ , however, does not vary systematically with depth but rather shows a step function, with a discontinuity at 6 m depth (Fig. 5). Such a trend has been explained by Rayleigh distillation during intense weathering for samples above 6 m depth and by mixing between an isotopically light saprolite and heavy groundwater for samples below 6 m depth (Rudnick et al., 2004). The

extremely light sample at 6 m discontinuity remains enigmatic. The complex behaviors of Li isotopes may reflect a mineralogical control on Li isotope fractionation in the saprolite (Rudnick et al., 2004). For example, with the increasing weathering intensity, the K/S ratio increases in samples below the 2 m discontinuity, coupled with a decrease of Li and  $\delta^7\text{Li}$  (Fig. 6). Samples above the 2 m discontinuity have the lowest K/S ratio, lowest Li concentration, medium  $\delta^7\text{Li}$  value (Fig. 6), lowest kaolinite and smectite content, and the highest  $\text{Fe}_2\text{O}_3$  content (Gardner et al., 1981). The coupled variations of kaolinite and smectite with Li and  $\delta^7\text{Li}$  values suggest a preference of Li in smectite over kaolinite and a difference in Li isotopic composition between kaolinite and smectite. This agrees with previous studies that showed that uptake of Li into smectite doesn't fractionate Li isotopes (Zhang et al., 1998), whereas uptake into kaolinite will (Pistiner and Henderson, 2003).

In addition, recent advances related to diffusion-driven Li isotope fractionation make it possible to explore the possibility of interpreting the complex behavior of Li isotopes in the saprolite profile by involving Li diffusion. The peculiar trend of  $\delta^7\text{Li}$  with depth in the saprolite profile can be modeled by a two-step process: equilibrium isotope fractionation during continental weathering, followed by kinetic isotope fractionation during diffusively-driven redistribution of the Li in the saprolite.

Lithium is fluid-mobile and is released into the water during continental weathering, with  $^7\text{Li}$  preferring fluids to rocks (Huh et al., 2004; Kisakurek et al., 2004, 2005; Pistiner and Henderson, 2003; Pogge Von Strandmann et al., 2008b; Rudnick et al., 2004). As a result, Li and  $\delta^7\text{Li}$  values in the saprolite profile are expected to decrease as weathering increases towards the surface. Loss of heavy Li during weathering is supported by the observation that all saprolites have  $\delta^7\text{Li}$  values lower than the unweathered diabase. The downward transports of leached Li from above and a possible water table at 6 m depth may have led to an increased Li concentration in the rocks below the water table and resulted in upward diffusion of Li across the 6 m boundary, possibly in water wicked into capillaries above the water table. This upward diffusion of Li was attended by kinetic isotope fractionation, which can be very large during diffusion of Li

(e.g., Aulbach and Rudnick, 2009; Jeffcoate et al., 2007; Lundstrom et al., 2005; Marks et al., 2007; Parkinson et al., 2007; Richter et al., 2003; Teng et al., 2006; X.-M. Liu et al., 2010).

The diffusion is modeled as a two-dimensional process, with  $^6\text{Li}$  and  $^7\text{Li}$  profiles modeled separately, following similar methods outlined by Teng et al. (2006). The best fit for the Li concentration and  $\delta^7\text{Li}$  data of the saprolites (Fig. 5) results in the following values:  $Dt = 0.5 \text{ (m}^2\text{)}$  where  $D =$  diffusion coefficient and  $t =$  the duration of the diffusion process; the upper and lower portions of the saprolite profiles have the initial Li concentrations of 9 ppm and 50 ppm, respectively, with a homogenous  $\delta^7\text{Li} = -12$  (weathering is unlikely to have resulted in an initial homogenous profile with respect to Li and  $\delta^7\text{Li}$  values, but we make this assumption in order to simplify the modeling). The  $\beta$  value, which is defined from the ratio of the relative diffusivities of the two isotopes:  $D^6_{\text{Li}}/D^7_{\text{Li}} = (m^7_{\text{Li}}/m^6_{\text{Li}})^\beta$ , is equal to 0.18. It is worth noting that these values are not unique and can vary slightly within the data limits of the saprolite profile.

Although neither the effective diffusion coefficient ( $D$ ) nor the duration of the diffusion process ( $t$ ) are known, the minimum  $D$  can be calculated by assuming that the maximum time of diffusion is equal to the age of the saprolites. Although the exact age of the saprolites is uncertain, based on the saprolite geometry and soil development, Pavich and Obermeier (1985) suggested that the saprolites developed after the Miocene. If we assume the maximum age of the saprolites is 23 Ma, then the minimum  $D_{\text{saprolite}}$  for Li is calculated to be  $\sim 7 \times 10^{-12} \text{ cm}^2/\text{s}$ . This estimated minimum  $D$  value is at least  $>2$  orders of magnitude higher than those measured in silicate minerals (e.g., feldspar and pyroxene) at temperatures of  $>800^\circ\text{C}$  (Coogan et al., 2005; Giletti and Shanahan, 1997) but is similar to  $D$ 's inferred for fluid-infiltrated amphibolites ( $2 \times 10^{-12} \text{ cm}^2/\text{s}$ ) and schists ( $2 \times 10^{-11} \text{ cm}^2/\text{s}$ ) at temperatures of  $\geq \sim 350^\circ\text{C}$  (Teng et al., 2006). These results rule out the possibility of solid-state diffusion as the mechanism for Li diffusion in the saprolites, but suggest diffusion might have occurred in an interconnected fluid phase that interacted with secondary mineral grains. In addition, the inferred  $\beta$  value of 0.18 is similar to those inferred for fluid-infiltrated amphibolite and schist (0.12 to 0.15) (Teng et al., 2006), but is greater than those measured in water (0.071 and 0.015, Fritz (1992) and Richter et al. (2006), respectively). This further suggests that diffusion of Li in the saprolites occurred along fluid-filled grain-boundaries, the same mechanism that produced Li diffusion profiles in country rocks of the Tin Mountain pegmatite (Teng et al., 2006). It is worth noting that our modeling cannot rule out the possibility of transport of Li through both diffusion and advection via aqueous fluid, as in this case the apparent  $D$  value would be even larger, as shown by X.-M. Liu et al. (2010).

It is unclear why Li isotopes were fractionated by diffusion in the saprolite profile while Mg isotopes were not. Lithium diffuses slightly slower than Mg in pure  $\text{H}_2\text{O}$  (Leaist and Kanakos, 2000; Richter et al., 2006) but considerably faster than Mg in silicate minerals (Brady, 1995). Furthermore, Li isotopes can be significantly fractionated during diffusion in water, whereas Mg isotopes cannot (Richter et al., 2006). Both of these factors may contribute to the different behaviors between Li and Mg in the saprolite. Nonetheless, the modeling presented above suggests that diffusion-driven kinetic isotope fractionation of Li can occur not only during high-temperature geological processes (e.g., Jeffcoate et al., 2007; Lundstrom et al., 2005; Marks et al., 2007; Parkinson et al., 2007; Teng et al., 2006; X.-M. Liu et al., 2010) but also likely during water–rock interactions at low temperatures.

### 5.3. Implications for the Mg isotopic composition of the crust and mantle

Our studies indicate that Mg isotopes, like Li isotopes (e.g., Chan et al., 1992; Huh et al., 1998, 2001, 2004; Kisakurek et al., 2004, 2005; Pistiner and Henderson, 2003; Pogge Von Strandmann et al., 2008b;

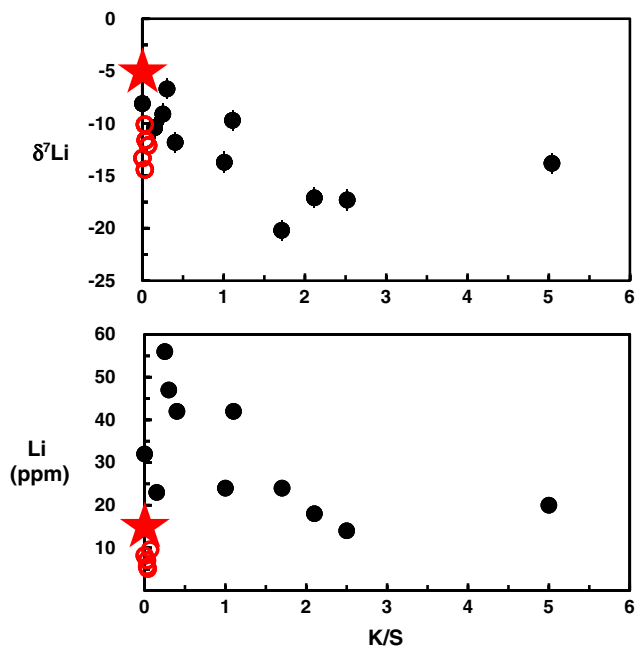


Fig. 6. K/S (kaolinite/smectite) ratio vs. Li concentration and isotopic composition. Star represents unweathered diabase; and open circles represent samples at or above 2 m depth and closed circles are samples below 2 m. Data are reported in Table 2.

Rudnick et al., 2004), Ca isotopes (e.g., Fantle and DePaolo, 2007; Jacobson and Holmden, 2008; Tipper et al., 2006b, 2008) and Fe isotopes (e.g., Bergquist and Boyle, 2006; Fantle and DePaolo, 2004; Thompson et al., 2007), can be significantly fractionated during continental weathering. In comparison to Li isotopes, continental weathering releases light Mg into the hydrosphere and leaves isotopically heavy Mg behind in the weathered products – the opposite of what is observed for Li isotopes. Consequently, compared to the upper mantle, the hydrosphere, on average, becomes isotopically lighter, as shown in studies of rivers and seawater (Brenot et al., 2008; de Villiers et al., 2005; Pogge Von Strandmann et al., 2008a,b; Tipper et al., 2006a,b, 2008) and the continental crust, at least the upper continental crust, is inferred to be isotopically heavier.

This prediction is supported by recent studies of crustal rocks (shale, loess and granites), which have variable, but, on average, heavier Mg isotopic compositions compared to the mantle (Li et al., 2010; S.-A. Liu et al., 2010; Shen et al., 2009). It is further supported by a first-order calculation based on the global budget of Mg isotopes (Fig. 7). Given that Mg isotopes do not fractionate during igneous differentiation (Li et al., 2010; S.-A. Liu et al., 2010; Teng et al., 2007, 2010; Yang et al., 2009), juvenile crust and the mantle are assumed to have identical Mg isotopic compositions. Weathering will gradually modify Mg isotopic composition of the juvenile crust by yielding isotopically light Mg isotopes that are transferred to oceans via river and groundwater discharge. Assuming that the MgO content of the juvenile continental crust is ~10 wt.% (similar to juvenile arc basalts, Lee et al., 2008) with an initial mantle-like  $\delta^{26}\text{Mg}$  of  $-0.25$  (Handler et al., 2009; Teng et al., 2007, 2010; Yang et al., 2009) and that the present-day riverine Mg flux to the oceans of  $5.2 \times 10^{18}$  moles per million years (Wilkinson and Algeo, 1989) with an average  $\delta^{26}\text{Mg}$  of  $-1.09$  (Tipper et al., 2006c) is representative of the past flux, the Mg isotopic evolution of the continental crust as a result of weathering can be calculated (Fig. 7). The model is run in  $1 \times 10^8$  yr time steps for  $\sim 4.0 \times 10^9$  yr, when the

model continental crust composition meets the higher end of Mg isotopic composition of the present-day continental crustal rocks (Li et al., 2010; S.-A. Liu et al., 2010; Shen et al., 2009). Although this first-order calculation is clearly an oversimplification, the main conclusion, that Mg isotopic composition of the continental crust is clearly modified by weathering, is robust. It is also consistent with Li isotopic systematics, where the Li isotopic composition of the continental crust is clearly modified by weathering, as shown by both first-order modeling (Elliott et al., 2004) and studies of continental rocks (Qiu et al., 2009; Teng et al., 2004, 2008, 2009).

Compared to modeling the effects of weathering on the Mg isotopic composition of the continental crust, assessing the effects of subduction of altered oceanic crust on the Mg isotopic composition of the mantle is difficult, since the Mg isotopic composition of altered oceanic crust is still unknown. However, it is still possible to evaluate this indirectly by assuming a steady-state Mg isotopic composition for the oceans: if seawater has a constant Mg isotopic composition, then the Mg flux from continents to the oceans must balance the flux to the oceanic crust (Fig. 7), which is eventually subducted into the mantle via subduction. Following the approach used above for studying the effects of weathering on the Mg isotopic composition of continental crust and assuming that the MgO content of the upper mantle is 37.8 wt.% (McDonough and Sun, 1995) with an initial  $\delta^{26}\text{Mg}$  of  $-0.25$  (Handler et al., 2009; Teng et al., 2007, 2010; Yang et al., 2009), the Mg isotopic evolution of the upper mantle as a result of subduction can be calculated (Fig. 7). Although the subducted Mg has a lighter isotopic composition than the mantle, the magnitude of this light, recycled flux is not sufficient to shift the Mg isotopic composition of the upper mantle due to the fact that  $>99.9$  wt.% of Mg in the bulk Earth lies within the mantle, while Mg in the crust and hydrosphere is  $<0.1$  wt.%.

## 6. Conclusions

The main conclusions from this study are:

1. As the intensity of weathering increases from the bottom of the profile towards the surface, Mg concentrations gradually decrease and  $\delta^{26}\text{Mg}$  consistently increases from  $-0.22$  in the unweathered saprolite up to  $+0.65$  in saprolites near the surface.
2. Magnesium isotope fractionation, coupled with Mg loss during progressive weathering, can be modeled by Rayleigh distillation, with apparent fractionation factors between saprolites and the fluid ( $\alpha$ ) of 1.00005 to 1.0004, i.e., there is up to 0.4% fractionation in the  $^{26}\text{Mg}/^{24}\text{Mg}$  ratio between saprolite and fluid. The large variation in  $\alpha$  value reflects a mineralogical control on Mg isotope fractionation during primary dissolution of Mg-rich minerals and formation of secondary minerals during continental weathering.
3. In contrast to Mg isotopes, Li isotopes in the profile might reflect both chemical weathering and superimposed kinetic fractionation due to diffusion. The reasons for the contrasting behaviors between Li and Mg isotopes remain unclear but may reflect differences in their diffusivities and larger isotope fractionation of Li in fluids compared to Mg.
4. Continental weathering significantly fractionates Mg isotopes, releasing light Mg into the hydrosphere and leaving isotopically heavy Mg behind in the regolith – the opposite sense of Li isotope fractionation during weathering. We show that weathering will gradually shift Mg isotopic composition of the continental crust towards heavy values, whereas subduction recycling should not significantly modify the Mg isotopic composition of the mantle.
5. More studies on natural weathering profiles developed on different protoliths under various climate conditions and laboratory work on Mg isotope fractionation between fluids and minerals are needed in order to further understand the behavior of Mg isotopes during continental weathering.

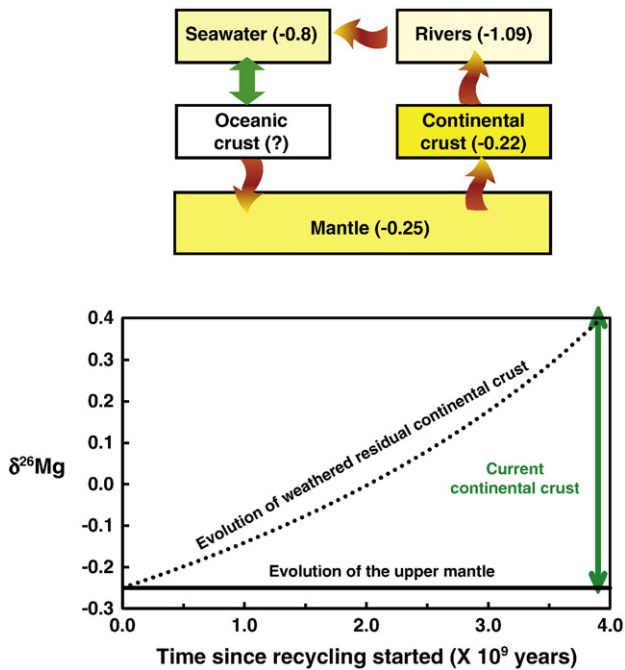


**Fig. 7.** Upper panel: cartoon showing the major components of the global Mg cycle with present-day  $\delta^{26}\text{Mg}$  values (in the parentheses). Light color of the component corresponds to light Mg isotopic composition. Lower panel: isotopic evolution of continental crust and upper mantle in response to removal of riverine Mg from the continental crust and its recycling into the mantle via subduction. The Mg isotopic composition of the present-day continental crustal rocks is from Shen et al. (2009), Li et al. (2010) and S.-A. Liu et al. (2010). See text for details.

## Acknowledgements

We thank John Dixon, Albert Galy, Lixin Jin, Shan Ke, Sheng-Ao Liu, Lin Ma, Wei Yang and an anonymous reviewer for comments on an earlier version. The paper benefited from constructive comments of Matt Fantle, Andy Jacobsen and Rachael James, and efficient editing from Rick Carlson. This work was supported by the National Science Foundation (EAR-0838227 to FZT; EAR 0208012 and EAR 0609689 to RLR) and Arkansas Space Grant Consortium (SW19002) to FZT.

## References

- Albarede, F., 1998. The growth of continental crust. *Tectonophysics* 296, 1–14.
- Anderson Jr., A.T., 1982. Parental basalts in subduction zones: implications for continental evolution. *J. Geophys. Res.* 87 (B8), 7047–7060.
- Aulbach, S., Rudnick, R.L., 2009. Origins of non-equilibrium lithium isotopic fractionation in xenolithic peridotite minerals: examples from Tanzania. *Chem. Geol.* 258, 17–27.
- Bergquist, B.A., Boyle, E.A., 2006. Iron isotopes in the Amazon River system: weathering and transport signatures. *Earth Planet. Sci. Lett.* 248 (1–2), 54–68.
- Berner, E.K., Berner, R.A., 1987. *The Global Water Cycle*. Prentice-Hall, Upper Saddle River, NJ, 397 pp.
- Brady, J.B., 1995. Diffusion data for silicate minerals, glasses, and liquids. In: Ahrens, T.H. (Ed.), *Mineral Physics and Crystallography: A Handbook of Physical Constants*. American Geophysical Union, Washington, D. C., pp. 269–290.
- Brenot, A., Cloquet, C., Vigier, N., Carignan, J., France-Lanord, C., 2008. Magnesium isotope systematics of the lithologically varied Moselle river basin, France. *Geochim. Cosmochim. Acta* 72, 5070–5089.
- Chan, L.H., Edmond, J.M., 1988. Variation of lithium isotope composition in the marine-environment: a preliminary report. *Geochim. Cosmochim. Acta* 52 (6), 1711–1717.
- Chan, L.H., Edmond, J.M., Thompson, G., Gillis, K., 1992. Lithium isotopic composition of submarine basalts: implications for the lithium cycle in the oceans. *Earth Planet. Sci. Lett.* 108 (1–3), 151–160.
- Chang, V.T.-C., Makishima, A., Belshaw, N.S., O'Nions, R.K., 2003. Purification of Mg from low-Mg biogenic carbonates for isotope ratio determination using multiple collector ICP-MS. *J. Anal. At. Spectrom.* 18, 296–301.
- Coogan, L.A., Kasemann, S.A., Chakraborty, S., 2005. Rates of hydrothermal cooling of new oceanic upper crust derived from lithium-geospeedometry. *Earth Planet. Sci. Lett.* 240 (2), 415–424.
- Dauphas, N., Teng, F.-Z., Arndt, N.T., 2010. Magnesium and iron isotopes in 2.7 Ga Alexo komatiites: mantle signatures, no evidence for Soret diffusion, and identification of diffusive transport in zoned olivine. *Geochim. Cosmochim. Acta* 74, 3274–3291.
- de Villiers, S., Dickson, J.A.D., Ellam, R.M., 2005. The composition of the continental river weathering flux deduced from seawater Mg isotopes. *Chem. Geol.* 216 (1–2), 133–142.
- Drever, J.I., 1997. *The Geochemistry of Natural Waters: Surface and Groundwater Environments*. Prentice Hall, 436 pp.
- Edmond, J.M., Measures, C., McDuff, R.E., Chan, L.H., Collier, R., Grant, B., Gordon, L.L., Corliss, J.B., 1979. Ridge crest hydrothermal activity and the balances of the major and minor elements in the ocean: the Galapagos data. *Earth Planet. Sci. Lett.* 46 (1), 1–18.
- Elliott, T., Jeffcoate, A.B., Bouman, C., 2004. The terrestrial Li isotope cycle: light-weight constrains on mantle convection. *Earth Planet. Sci. Lett.* 220, 231–245.
- Fantle, M.S., DePaolo, D.J., 2004. Iron isotopic fractionation during continental weathering. *Earth Planet. Sci. Lett.* 228, 547–562.
- Fantle, M.S., DePaolo, D.J., 2007. Ca isotopes in carbonate sediment and pore fluid from ODP Site 807A: the  $\text{Ca}^{2+}$ (aq)-calcite equilibrium fractionation factor and calcite recrystallization rates in Pleistocene sediments. *Geochim. Cosmochim. Acta* 71 (10), 2524–2546.
- Flesch, G.D., Anderson, A.R.J., Svec, H.J., 1973. A secondary isotopic standard for  $^6\text{Li}/^7\text{Li}$  determinations. *Int. J. Mass Spectrom. Ion Processes* 12, 265–272.
- Fritz, S.J., 1992. Measuring the ratio of aqueous diffusion coefficients between  $^6\text{Li}^+$  and  $^7\text{Li}^+$  by osmometry. *Geochim. Cosmochim. Acta* 56 (10), 3781–3789.
- Galy, A., Yoffe, O., Janney, P.E., Williams, R.W., Cloquet, C., Alard, O., Halicz, L., Wadhwa, M., Hutcheon, I.D., Ramon, E., Carignan, J., 2003. Magnesium isotope heterogeneity of the isotopic standard SRM980 and new reference materials for magnesium-isotope-ratio measurements. *J. Anal. At. Spectrom.* 18 (11), 1352–1356.
- Gardner, L.R., Kheoruenromne, I., 1980. Siderite veins in saprolite, Cayce, South Carolina. *South Carolina Geology* 24 (1), 29–31.
- Gardner, L.R., Kheoruenromne, I., Chen, H.S., 1981. Geochemistry and mineralogy of an unusual diabase saprolite near Columbia, South Carolina. *Clays Clay Miner.* 29 (3), 184–190.
- Giletti, B.J., Shanahan, T.M., 1997. Alkali diffusion in plagioclase feldspar. *Chem. Geol.* 139 (1–4), 3–20.
- Goldich, S.S., 1938. A study in rock weathering. *J. Geol.* 46, 17–58.
- Handler, M.R., Baker, J.A., Schiller, M., Bennett, V.C., Yaxley, G.M., 2009. Magnesium stable isotope composition of Earth's upper mantle. *Earth Planet. Sci. Lett.* 282, 306–313.
- Huh, Y., Chan, L.-H., Zhang, L., Edmond, J.M., 1998. Lithium and its isotopes in major world rivers: implications for weathering and the oceanic budget. *Geochim. Cosmochim. Acta* 62 (12), 2039–2051.
- Huh, Y., Chan, L.-H., Edmond, J.M., 2001. Lithium isotopes as a probe of weathering processes: Orinoco River. *Earth Planet. Sci. Lett.* 194 (1–2), 189–199.
- Huh, Y., Chan, L.H., Chadwick, O.A., 2004. Behavior of lithium and its isotopes during weathering of Hawaiian basalt. *Geochim. Geophys. Geosyst.* 5 (9), Q09002. doi:10.1029/2004GC000729.
- Jacobson, A.D., Holmden, C., 2008.  $\delta^{44}\text{Ca}$  evolution in a carbonate aquifer and its bearing on the fractionation factor for calcite. *Earth Planet. Sci. Lett.* 270, 349–353.
- Jeffcoate, A., Elliott, T., Kasemann, S.A., Ionov, D.A., Cooper, K., Brooker, R., 2007. Li isotope fractionation in peridotites and mafic melts. *Geochim. Cosmochim. Acta* 71, 202–218.
- Kisakurek, B., Widdowson, M., James, R.H., 2004. Behaviour of Li isotopes during continental weathering: the Bidar laterite profile, India. *Chem. Geol.* 212 (1–2), 27–44.
- Kisakurek, B., James, R.H., Harris, N.B.W., 2005. Li and delta Li-7 in Himalayan rivers: proxies for silicate weathering? *Earth Planet. Sci. Lett.* 237 (3–4), 387–401.
- Kump, L.R., Brantley, S.L., Arthur, M.A., 2000. Chemical weathering, atmospheric  $\text{CO}_2$  and climate. *Annu. Rev. Earth Planet. Sci.* 28, 611–667.
- Leaist, D.G., Kanakos, M.A., 2000. Measured and predicted ternary diffusion coefficients for concentrated aqueous  $\text{LiCl} + \text{KCl}$  solutions over a wide range of compositions. *Phys. Chem. Chem. Phys.* 2, 1015–1021.
- Lee, C.-T.A., Morton, D.M., Little, M.G., Kistler, R., Horodysky, U., Leeman, W.P., Agraniar, A., 2008. Regulating continent growth and composition by chemical weathering. *Proc. Natl Acad. Sci.* 105, 4981–4984.
- Li, Y.H., 1982. A brief discussion on the mean oceanic residence time of elements. *Geochim. Cosmochim. Acta* 46 (12), 2671–2675.
- Li, W.-Y., Teng, F.-Z., Ke, S., Rudnick, R.L., Gao, S., Wu, F.-Y., Chappell, B.W., 2010. Heterogeneous magnesium isotopic composition of the upper continental crust. *Geochim. Cosmochim. Acta*. doi:10.1016/j.gca.2010.08.030.
- Liu, S.-A., Teng, F.-Z., He, Y., Ke, S., Li, S., 2010. Investigation of magnesium isotope fractionation during granite differentiation: implication for Mg isotopic composition of the continental crust. *Earth Planet. Sci. Lett.* 297, 646–654.
- Liu, X.-M., Rudnick, R.L., Hier-Majumder, S., Sirbescu, M.-L.-C., 2010. Processes controlling lithium isotopic distribution in contact aureoles: a case study of the Florence County pegmatites, Wisconsin. *Geochim. Geophys. Geosyst.* 11, Q08014. doi:10.1029/2010GC003063.
- Lundstrom, C.C., Chaussidon, M., Hsui, A.T., Kelemen, P., Zimmerman, M., 2005. Observations of Li isotopic variations in the Trinity Ophiolite: evidence for isotopic fractionation by diffusion during mantle melting. *Geochim. Cosmochim. Acta* 69 (3), 735–751.
- Magna, T., Wiechert, U., Halliday, A.N., 2006. New constraints on the lithium isotope compositions of the Moon and terrestrial planets. *Earth Planet. Sci. Lett.* 243, 336–353.
- Marks, M.A.W., Rudnick, R.L., McCammon, C., Venemann, T., Markl, G., 2007. Arrested kinetic Li isotope fractionation at the margin of the Ilimaussaq complex, South Greenland: evidence for open-system processes during final cooling of peralkaline igneous rocks. *Chem. Geol.* 246, 207–230.
- McDonough, W.F., Sun, S.S., 1995. The composition of the Earth. *Chem. Geol.* 120 (3–4), 223–253.
- Parkinson, I.J., Hammond, S.J., James, R.H., Rogers, N.W., 2007. High-temperature lithium isotope fractionation: insights from lithium isotope diffusion in magmatic systems. *Earth Planet. Sci. Lett.* 257, 609–621.
- Pavich, M.J., Obermeier, S.F., 1985. Saprolite formation beneath coastal-plain sediments near Washington, DC. *Geol. Soc. Am. Bull.* 96 (7), 886–900.
- Pistiner, J.S., Henderson, G.M., 2003. Lithium-isotope fractionation during continental weathering processes. *Earth Planet. Sci. Lett.* 214 (1–2), 327–339.
- Pogge Von Strandmann, P.A.E., Burton, K.W., James, R.H., Van Calstern, P., Gislason, S.R., Sigmarsson, O., 2008a. The influence of weathering processes on riverine magnesium isotopes in a basaltic terrain. *Earth Planet. Sci. Lett.* 276, 187–197.
- Pogge Von Strandmann, P.A.E., James, R.H., Van Calstern, P., Gislason, S.R., Burton, K.W., 2008b. Lithium, magnesium and uranium isotope behaviour in the estuarine environment of basaltic islands. *Earth Planet. Sci. Lett.* 274, 462–471.
- Qiu, L., Rudnick, R.L., McDonough, W.F., Merriman, R.J., 2009. Li and  $\delta^{7}\text{Li}$  in mudrocks from the British Caledonides: metamorphism and source influences. *Geochim. Cosmochim. Acta* 73 (24), 7325–7340.
- Richter, F.M., Davis, A.M., DePaolo, D.J., Watson, E.B., 2003. Isotope fractionation by chemical diffusion between molten basalt and rhyolite. *Geochim. Cosmochim. Acta* 67 (20), 3905–3923.
- Richter, F.M., Mendybaev, R.A., Christensen, J.N., Hutcheon, I.D., Williams, R.W., Sturchio, N.C., Beloso, J.A.D., 2006. Kinetic isotopic fractionation during diffusion of ionic species in water. *Geochim. Cosmochim. Acta* 70 (2), 277–289.
- Rudnick, R.L., Tomascak, P.B., Njo, H.B., Gardner, L.R., 2004. Extreme lithium isotopic fractionation during continental weathering revealed in saprolites from South Carolina. *Chem. Geol.* 212 (1–2), 45–57.
- Seitz, H.-M., Brey, G.P., Lahaye, Y., Durali, S., Weyer, S., 2004. Lithium isotopic signatures of peridotite xenoliths and isotopic fractionation at high temperature between olivine and pyroxenes. *Chem. Geol.* 212 (1–2), 163–177.
- Shen, B., Jacobsen, B., Lee, C.-T.A., Yin, Q.Z., Morton, D.M., 2009. The Mg isotopic systematics of granitoids in continental arcs and implications for the role of chemical weathering in crust formation. *Proc. Natl Acad. Sci.* 106, 20652–20657.
- Teng, F.-Z., McDonough, W.F., Rudnick, R.L., Dalpe, C., Tomascak, P.B., Chappell, B.W., Gao, S., 2004. Lithium isotopic composition and concentration of the upper continental crust. *Geochim. Cosmochim. Acta* 68 (20), 4167–4178.
- Teng, F.-Z., McDonough, W.F., Rudnick, R.L., Walker, R.J., 2006. Diffusion-driven extreme lithium isotopic fractionation in country rocks of the Tin Mountain pegmatite. *Earth Planet. Sci. Lett.* 243 (3–4), 701–710.
- Teng, F.-Z., Wadhwa, M., Helz, R.T., 2007. Investigation of magnesium isotope fractionation during basalt differentiation: implications for a chondritic composition of the terrestrial mantle. *Earth Planet. Sci. Lett.* 261 (1–2), 84–92.

- Teng, F.-Z., Rudnick, R.L., McDonough, W.F., Gao, S., Tomascak, P.B., Liu, Y., 2008. Lithium isotopic composition and concentration of the deep continental crust. *Chem. Geol.* 255, 47–59.
- Teng, F.-Z., Rudnick, R.L., McDonough, W.F., Wu, F.-Y., 2009. Lithium isotopic systematics of A-type granites and their mafic enclaves: further constraints on the Li isotopic composition of the continental crust. *Chem. Geol.* 262, 415–424.
- Teng, F.-Z., Li, W.-Y., Ke, S., Marty, B., Dauphas, N., Huang, S., Wu, F.-Y., Pourmand, A., 2010. Magnesium isotopic composition of the Earth and chondrites. *Geochim. Cosmochim. Acta* 74, 4150–4166.
- Thompson, A., Ruiz, J., Chadwick, O.A., Titus, M., Chorover, J., 2007. Rayleigh fractionation of iron isotopes during pedogenesis along a climate sequence of Hawaiian basalt. *Chem. Geol.* 238 (1–2), 72–83.
- Tipper, E.T., Bickle, M.J., Galy, A., West, A.J., Pomies, C., Chapman, H.J., 2006a. The short term climatic sensitivity of carbonate and silicate weathering fluxes: insight from seasonal variations in river chemistry. *Geochim. Cosmochim. Acta* 70 (11), 2737–2754.
- Tipper, E.T., Galy, A., Bickle, M.J., 2006b. Riverine evidence for a fractionated reservoir of Ca and Mg on the continents: implications for the oceanic Ca cycle. *Earth Planet. Sci. Lett.* 247 (3–4), 267–279.
- Tipper, E.T., Galy, A., Gaillardet, J., Bickle, M.J., Elderfield, H., Carder, E.A., 2006c. The magnesium isotope budget of the modern ocean: constraints from riverine magnesium isotope ratios. *Earth Planet. Sci. Lett.* 250, 241–253.
- Tipper, E.T., Galy, A., Bickle, M.J., 2008. Calcium and magnesium isotope systematics in rivers draining the Himalaya–Tibetan–Plateau region: lithological or fractionation control? *Geochim. Cosmochim. Acta* 72, 1057–1075.
- Urey, H.C., 1952. *The Planets: Their Origin and Development*. Yale University Press, New Haven, CT. 245 pp.
- Wiechert, U., Halliday, A.N., 2007. Non-chondritic magnesium and the origins of the inner terrestrial planets. *Earth Planet. Sci. Lett.* 256, 360–371.
- Wilkinson, B.H., Algeo, T.J., 1989. Sedimentary carbonate record of calcium–magnesium cycling. *Am. J. Sci.* 289, 1158–1194.
- Yang, W., Teng, F.-Z., Zhang, H.-F., 2009. Chondritic magnesium isotopic composition of the terrestrial mantle: a case study of peridotite xenoliths from the North China craton. *Earth Planet. Sci. Lett.* 288 (3–4), 475–482.
- Young, E.D., Galy, A., 2004. The isotope geochemistry and cosmochemistry of magnesium. In: Johnson, C.M., Beard, B.L., Albarede, F. (Eds.), *Geochemistry of Non-Traditional Stable Isotopes. Reviews in Mineralogy & Geochemistry*. Mineralogical Society of America, Washington D. C. pp. 197–230.
- Zhang, L., Chan, L.H., Gieskes, J.M., 1998. Lithium isotope geochemistry of pore waters from Ocean Drilling Program Sites 918 and 919, Irminger Basin. *Geochim. Cosmochim. Acta* 62 (14), 2437–2450.